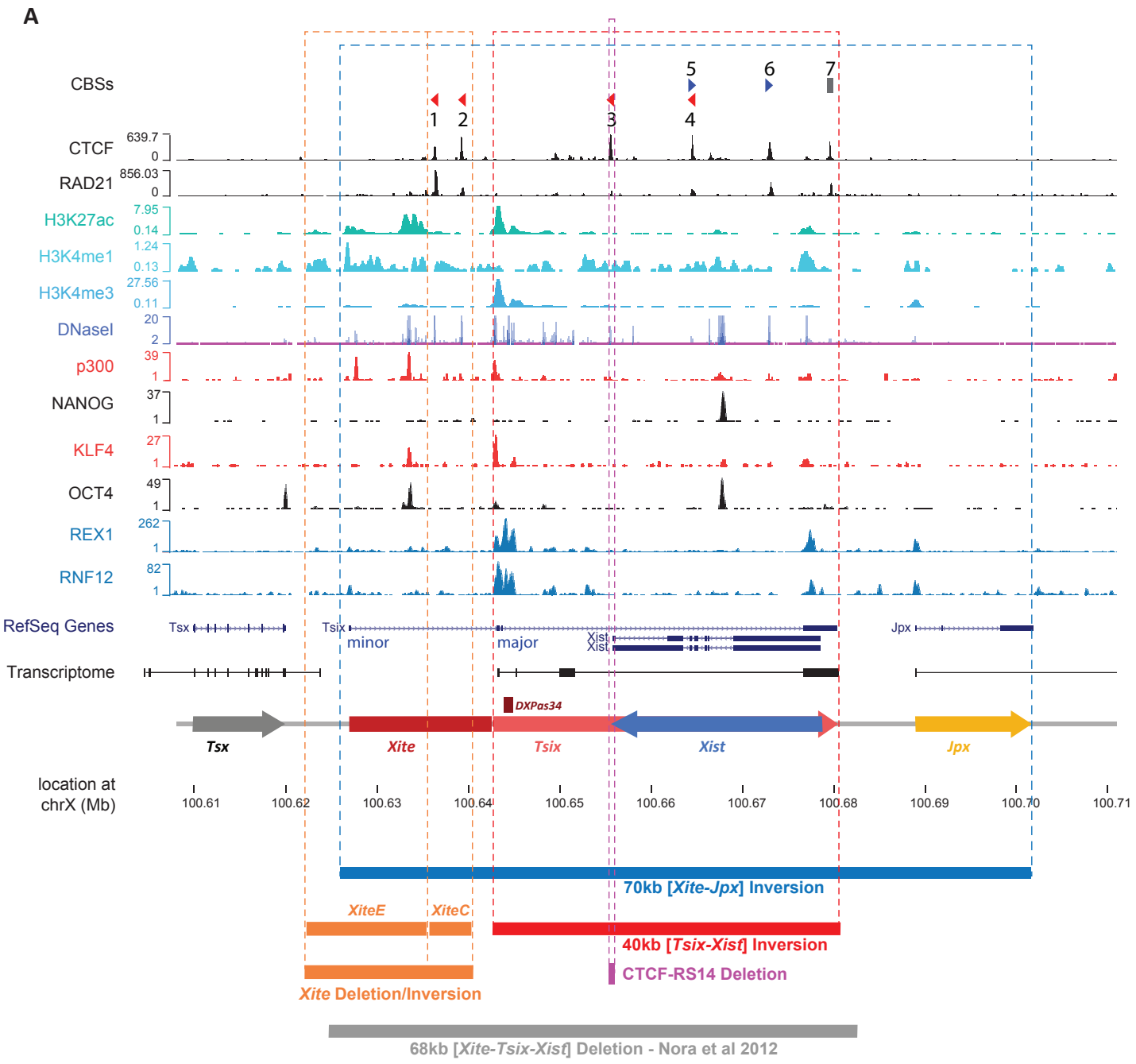
A
CBSs
1
2
3
4
5
6
7
CTCF
RAD21
H3K27ac
H3K4me1
H3K4me3
DNaseI
p300
NANOG
KLF4
OCT4
REX1
RNF12
RefSeq Genes
Tsx
Tsix
minor
major
Xist
Jpx
Transcriptome
DXPas34
Tsx
Xite
Tsix
Xist
Jpx
location at chrX (Mb)
100.61
100.62
100.63
100.64
100.65
100.66
100.67
100.68
100.69
100.70
100.71
70kb [Xite-Jpx] Inversion
XiteE
XiteC
40kb [Tsix-Xist] Inversion
CTCF-RS14 Deletion
Xite Deletion/Inversion
68kb [Xite-Tsix-Xist] Deletion - Nora et al 2012

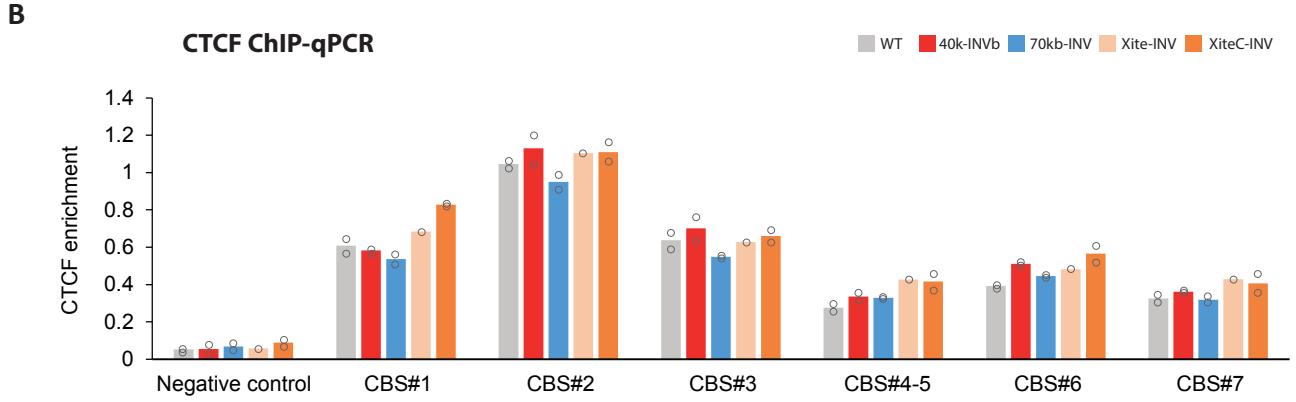
B
CTCF ChIP-qPCR
WT
40k-INVb
70kb-INV
Xite-INV
XiteC-INV
CTCF enrichment
1.4
1.2
1
0.8
0.6
0.4
0.2
0
Negative control
CBS#1
CBS#2
CBS#3
CBS#4-5
CBS#6
CBS#7

Supplementary Fig. 1:

A) Overview of chromatin features at the inverted or deleted regions in male mESCs: CRISPR-mediated mutations and inversions depicted with dashed boxes, 40kb [*Tsix-Xist*] inversion (red), 70kb [*Xite-Jpx*] inversion (blue), *Xite*-related deletions or inversions (orange) and CTCF deletion (purple). CTCF and RAD21 ChiP-seq in E14 mESCs (Nora, Goloborodko et al. 2017), H3K27ac, H3K4me1 and H3K4me3 ChiP-seq in E14 mESCs (Yue, Cheng et al. 2014)'(Consortium 2012), and DNaseI hypersensitivity in CJ7 mESCs (Yue, Cheng et al. 2014)'(Consortium 2012), p300 ChIP-seq in 129JAE-C57/B6 mESCs (Creyghton, Cheng et al. 2010), NANOG and OCT4 in V6.5 (C57BL/6-129) mESCs (Marson, Levine et al. 2008), KLF4 in E14 mESCs (Chen, Xu et al. 2008), and REX1 and RNF12 in F1 2-1 (129/Sv-Cast/Ei) mESCs (Gontan, Achame et al. 2012). Underneath, UCSC RefSeq gene annotation (Kent, Sugnet et al. 2002) and RNA-seq based transcriptome in V6.5 mESCs (Guttman, Garber et al. 2010), the annotations used in this paper (including Xite, see methods) and the genomic location (Mb) on the X chromosome in mm9. Tsix minor and major annotation from (Stavropoulos, Rowntree et al. 2005).

B) CTCF ChIP-qPCR results show no differences in CTCF binding within the inverted region between WT and INV cells. CTCF enrichment is relative to input and normalized to positive control, a CBS lying outside the X chromosome. Center values represent average of converted mean CT values from two independent clones for each genotype, except for Xite-INV. Mean CT values for each clone is an average from three technical replicates.

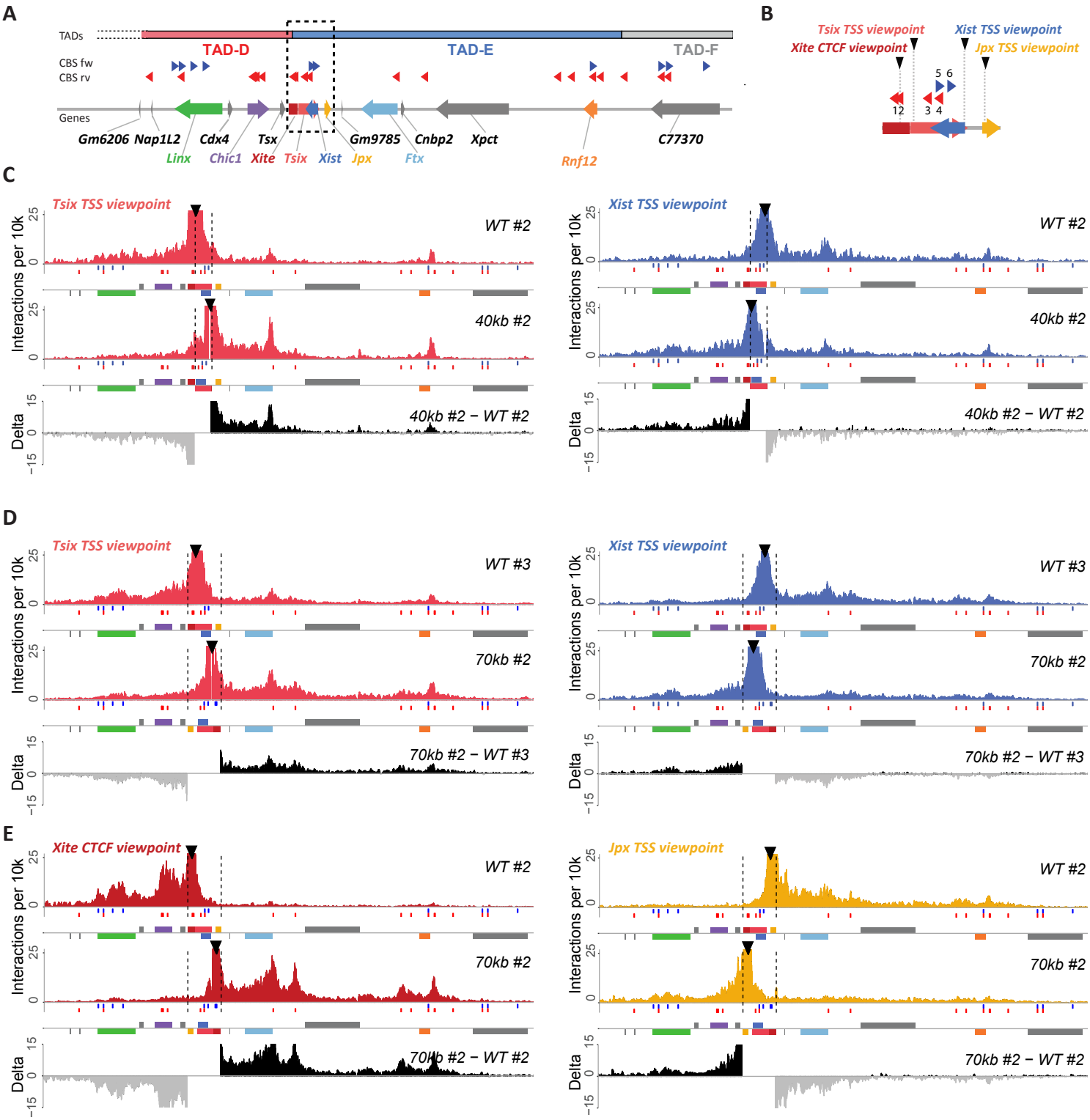
A
TADs
TAD-D
TAD-E
TAD-F
CBS fw
CBS rv
Genes
Gm6206 Nap1L2 Cdx4 Tsx Gm9785 Cnbp2 Xpct C77370
Linx Chic1 Xite Tsix Xist Jpx Ftx Rnf12
B
Tsix TSS viewpoint
Xite CTCF viewpoint
Xist TSS viewpoint
Jpx TSS viewpoint
5 6
12 3 4
C
Tsix TSS viewpoint
Xist TSS viewpoint
WT #2
40kb #2
40kb #2 − WT #2
Interactions per 10k
Delta
D
Tsix TSS viewpoint
Xist TSS viewpoint
WT #3
70kb #2
70kb #2 − WT #3
E
Xite CTCF viewpoint
Jpx TSS viewpoint
WT #2
70kb #2
70kb #2 − WT #2

F

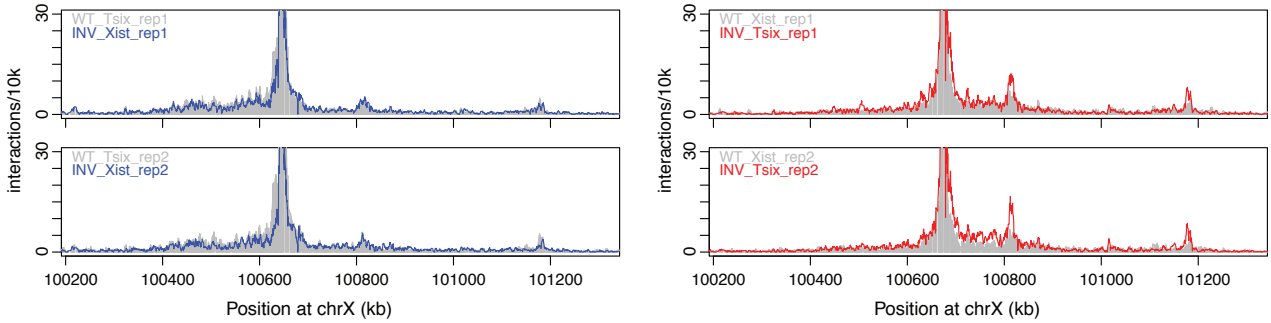
WT_Tsix_rep1
INV_Xist_rep1
WT_Tsix_rep2
INV_Xist_rep2
interactions/10k
0
30
100200
100400
100600
100800
101000
101200
Position at chrX (kb)
WT_Xist_rep1
INV_Tsix_rep1
WT_Xist_rep2
INV_Tsix_rep2
interactions/10k
0
30
100200
100400
100600
100800
101000
101200
Position at chrX (kb)

G

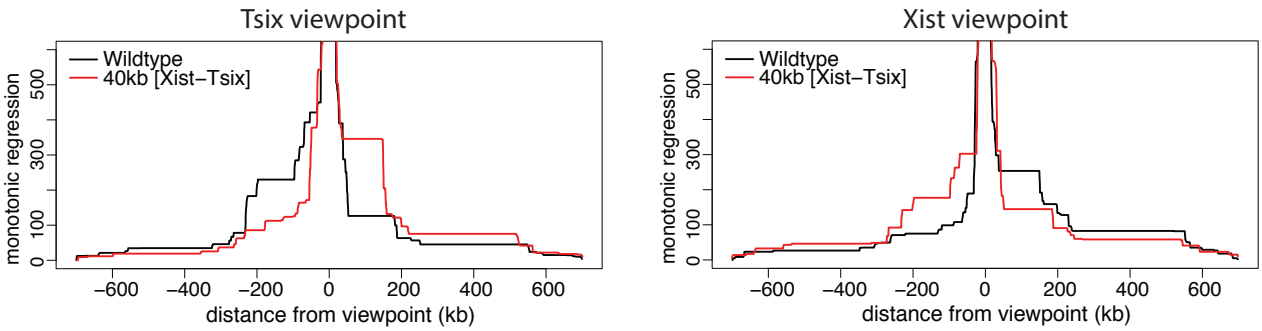
Tsix viewpoint
Wildtype
40kb [Xist−Tsix]
monotonic regression
0
100
300
500
−600
−400
−200
0
200
400
600
distance from viewpoint (kb)
Xist viewpoint
Wildtype
40kb [Xist−Tsix]
monotonic regression
0
100
300
500
−600
−400
−200
0
200
400
600
distance from viewpoint (kb)

Supplementary Fig. 2:

Note: Each inversion has been generated twice in independent cell lines. Capture-C results for the second clones are shown here, results for the first clones are shown in Figure 1-2.

A) TAD-D and -E as in Fig. 1B. Dashed box represents zoom-in in B.

B) Zoom-in of dashed box in A. Probes for capture enrichment (viewpoint) depicted with arrowheads. *Xite* viewpoint at CTCF site and *Xist*, *Tsix* and *Jpx* viewpoints at transcription start sites. CBSs in blue (forward) and red (reverse).

C) Capture-C profiles for *Tsix* (red) and *Xist* (blue) viewpoints in wild type and 40kb [*Tsix-Xist*] inversion. Profiles represent number of interactions for each DpnII fragment per 10,000 total interactions within the analyzed region (chrX:100214149-101420149), smoothened with a running mean of 7 DpnII fragments. Underneath the profiles, forward CBSs in blue, reverse CBSs in red and genes are annotated by colored boxes as in A, forward-oriented genes above and reverse-oriented genes below the grey line. Differential interaction frequencies of wild type minus inversion interaction frequencies are depicted in black (interaction gain) and grey (interaction loss).

D) Capture-C profiles and differential interaction frequencies, as in C, for *Tsix* (red) and *Xist* (blue) viewpoints in wild type and 70kb [*Xite-Jpx*] inversion.

E) Capture-C profiles and differential interaction frequencies, as in C, for *Xite* (dark red) and *Jpx* (yellow) viewpoints in wild type and 70kb [*Xite-Jpx*] inversion.

F) Capture-C profiles of 40kb inverted *Xist* (blue) and 40kb inverted *Tsix* (red) imposed on Capture-C profiles of respectively wildtype *Tsix* (grey) and wildtype *Xist* (grey). Capture-C profiles are represented as in C.

G) Monotonic regression model of the Capture-C signal is calculated using peakC (Geeven, Teunissen et al. 2018) (de Leeuw 2009) and plotted as a function of the distance to the *Tsix* and *Xist* viewpoint, for wildtype (black) compared to 40kb[*Tsix-Xist*] inverion. (red).

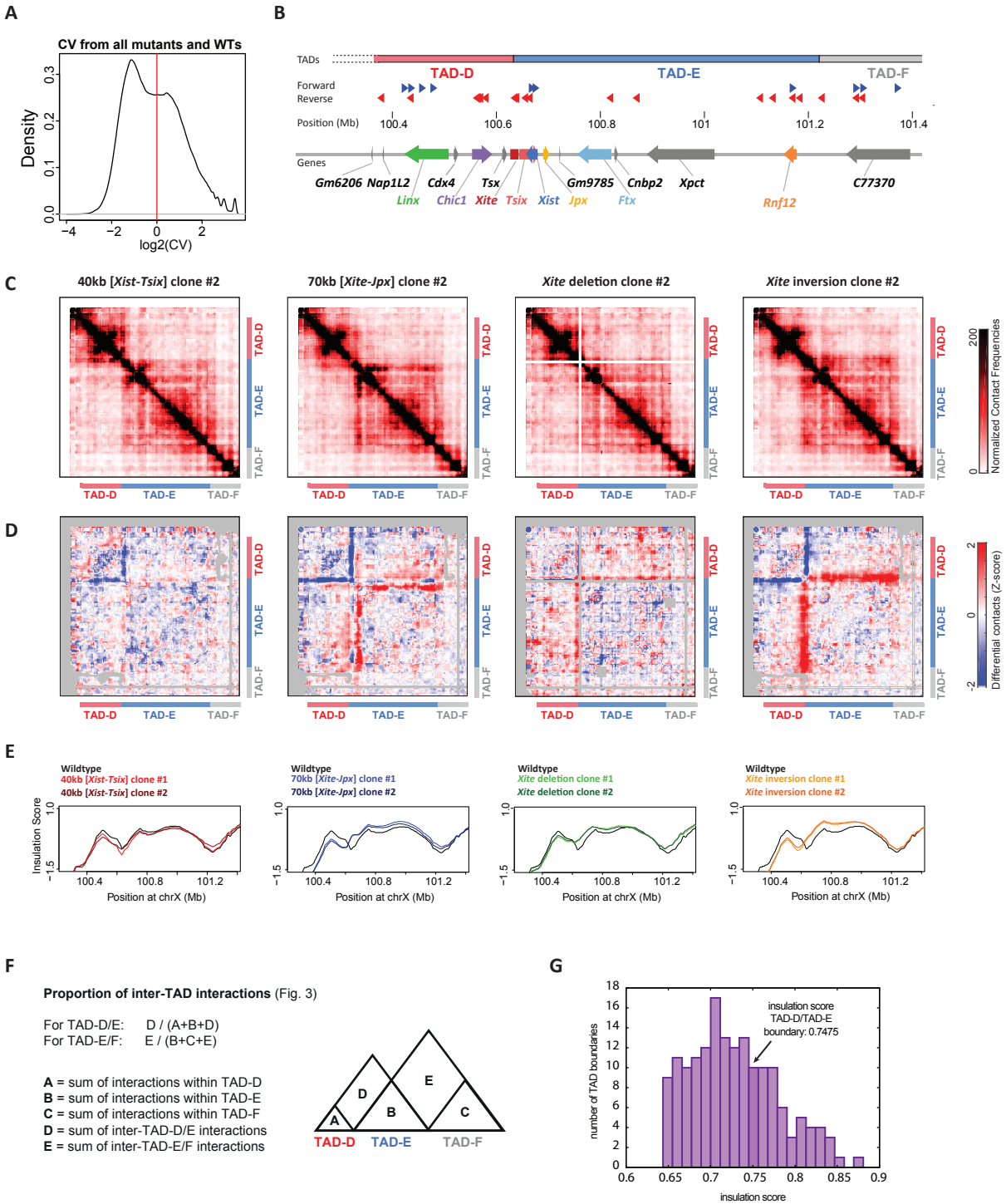

F

Proportion of inter-TAD interactions (Fig. 3)

For TAD-D/E: D / (A+B+D)
For TAD-E/F: E / (B+C+E)

A = sum of interactions within TAD-D
B = sum of interactions within TAD-E
C = sum of interactions within TAD-F
D = sum of inter-TAD-D/E interactions
E = sum of inter-TAD-E/F interactions

G

Supplementary Fig. 3:

A) Distribution of the coefficient of variation (CV) of interactions (pixels in the 5C map) in a 10x10 square centered on every interaction for all 5C samples. Red line indicates applied threshold of CV=1 (See Methods), chosen based on bimodal distribution.

B-E) 5C results for the second independent cell line of each genomic alteration. Results for the first clones are shown in main Fig. 1-2.

B) Linear visualization of the *Xic* organized into two TADs as in Fig. 1. TAD boundaries are determined using the insulation score, according to (Crane, Bian et al. 2015). Dotted lines at start of TAD-D indicate undefined TAD structure due to repetitive sequences. CTCF bound sequence motifs (CBSs) in forward (blue) and reverse (red) orientation (Nora, Goloborodko et al. 2017). Gene annotation from UCSC RefSeq mm9 (Kent, Sugnet et al. 2002), except for *Xite* (see Methods) and *Linx* (Nora, Lajoie et al. 2012).

C) 5C chromosome conformation contact frequencies in male mESCs harboring a 40kb [*Tsix-Xist*] inversion, 70kb [*Xite-Jpx*] inversion, *Xite* deletion or *Xite* inversion. Pools of two replicates, data has been inverted accordingly (i.e. maps represent the inverted genome), normalized and binned as in Fig. 1-2.

D) Differential 5C maps of mutant versus wild type mESCs. Differential maps represent the subtraction of wild type Z-scores from mutant Z-scores (see Methods). Gray pixels correspond to interactions that were filtered because they did not meet the quality control threshold (see Methods).

E) Insulation scores calculated according to (Crane, Bian et al. 2015). Wild type in black, 40kb [*Tsix-Xist*] inversion in red, 70kb [*Xite-Jpx*] inversion in blue, *Xite* deletion in green and *Xite* inversion in orange. Insulation scores for both clones are shown in the same graph.

F) Supporting figure for Fig. 3C, depicting the calculations of the proportion of inter-TAD interactions.

G) Distribution of insulation scores for TAD boundaries on the X chromosome. The reciprocal insulation score (Zhan, Mariani et al. 2017) was calculated for each TAD boundary using a published Hi-C dataset of mESCs (Giorgetti, Lajoie et al. 2016). The position of TADs and their boundaries on the X chromosome was determined using the CaTCH algorithm with a reciprocal insulation score of 65%.(Zhan, Mariani et al. 2017) The insulation score for the TAD-D/TAD-E boundary (indicated) is above the median.

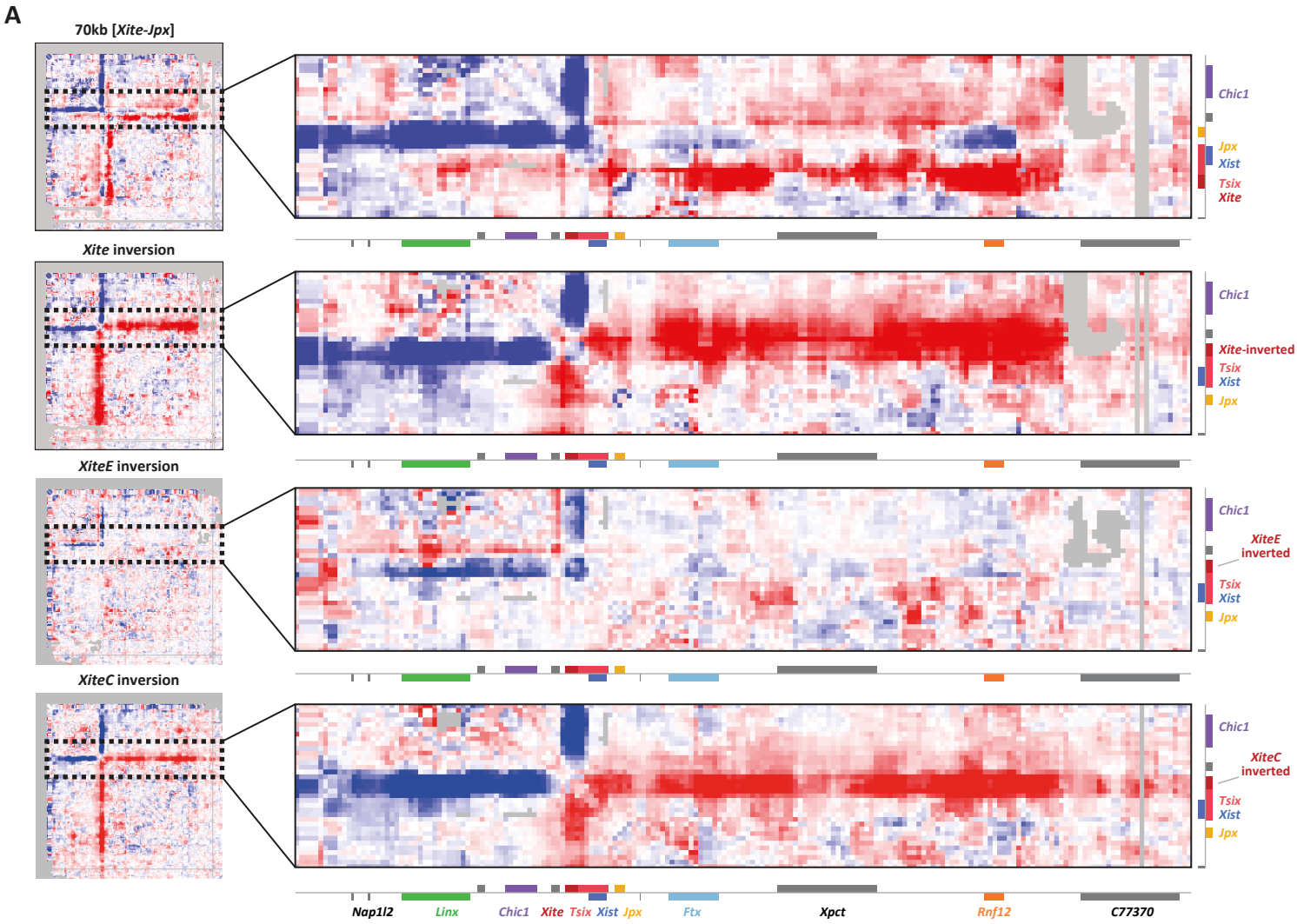
A
70kb [Xite-Jpx]
Xite inversion
XiteE inversion
XiteC inversion
Chic1
Jpx
Xist
Tsix
Xite
Xite-inverted
XiteE inverted
XiteC inverted
Nap1l2
Linx
Chic1
Xite
Tsix
Xist
Jpx
Ftx
Xpct
Rnf12
C77370

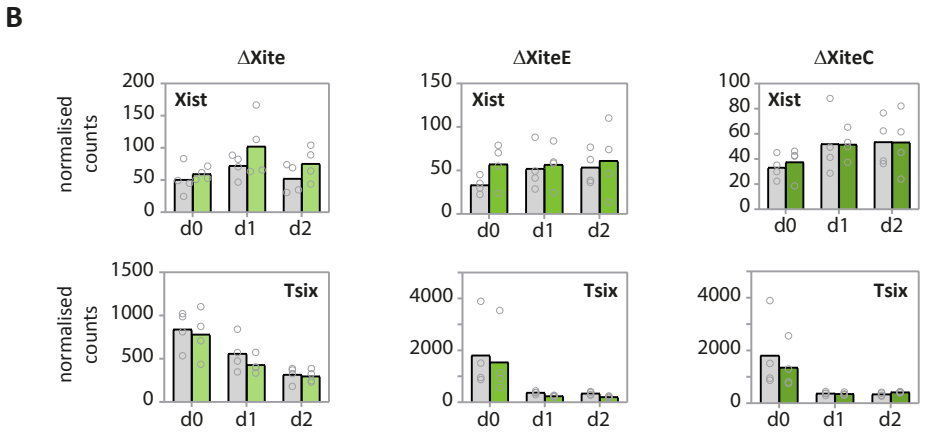
B
ΔXite
ΔXiteE
ΔXiteC
normalised counts
Xist
Tsix
d0
d1
d2

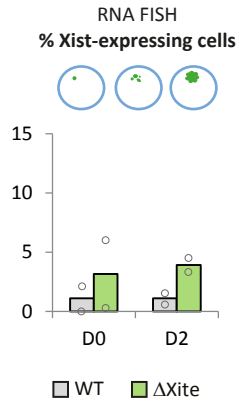
C
RNA FISH
% Xist-expressing cells
D0
D2
WT
ΔXite

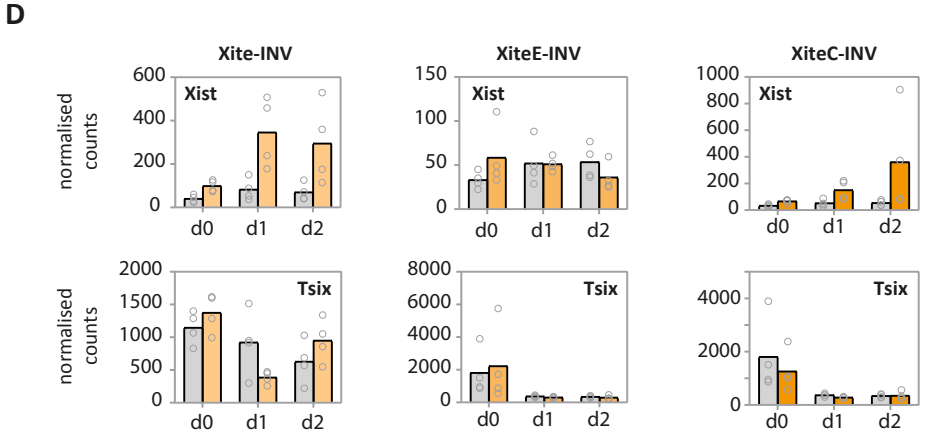
D
Xite-INV
XiteE-INV
XiteC-INV
normalised counts
Xist
Tsix
d0
d1
d2

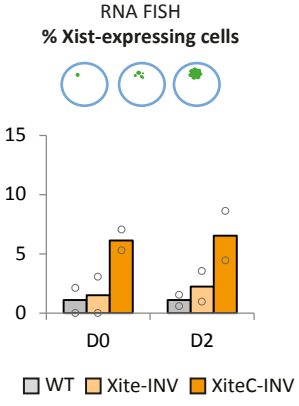
E
RNA FISH
% Xist-expressing cells
D0
D2
WT
Xite-INV
XiteC-INV

Supplementary Fig. 4:

A) Zoom-ins of differential 5C maps shown in Fig. 2F, 3G and 3J. Differential maps represent the subtraction of wild type Z-scores from mutant Z-scores (see Methods). Gray pixels correspond to interactions that were filtered because they did not meet the quality control threshold (see Methods).

B) nCounter® mRNA expression levels in Δ*Xite,* Δ*XiteE* and Δ*XiteC.* Wildtype samples for Δ*Xite* versus Δ*XiteE/*Δ*XiteC* are different because they were processed in different batches. Bars depict the mean of four biologically independent samples.

C) *Xist* expression analyzed by RNA-FISH in male wild type (grey) and Δ*Xite* (green) mESCs at day 0 or 2 of EpiLSC differentiation. We did not consider cells in which we could not detect either *Huwe1* (X-linked) or *Xist* expression. *Xist* expression was scored based on the presence of transcript pinpoint, accumulation or clouds. Bars represent the average percentage of counted cells in two independent replicates (n>100 cells for each replicate) (Supplementary Table 6 for exact sample size details).

D) nCounter® mRNA expression levels in *Xite, XiteE* and *XiteC* inversions. Wildtype samples for *Xite*-inversion versus *XiteE/XiteC*-inversions are different because they were processed in different batches. Bars depict the mean of four biologically independent samples.

E) *Xist* expression analyzed by RNA-FISH in male wild type (grey), *Xite*-inversion (yellow) and *XiteC*-inversion (orange) mESCs at day 0 or 2 of EpiLSC differentiation. We did not consider cells in which we could not detect neither *Huwe1* (X-linked) nor *Xist* expression. *Xist* expression was scored based on the presence of transcript pinpoint, accumulation or clouds. Bars represent the average percentage of counted cells in two independent replicates (n>100 cells for each replicate) (Supplementary Table 6 for exact sample size details).

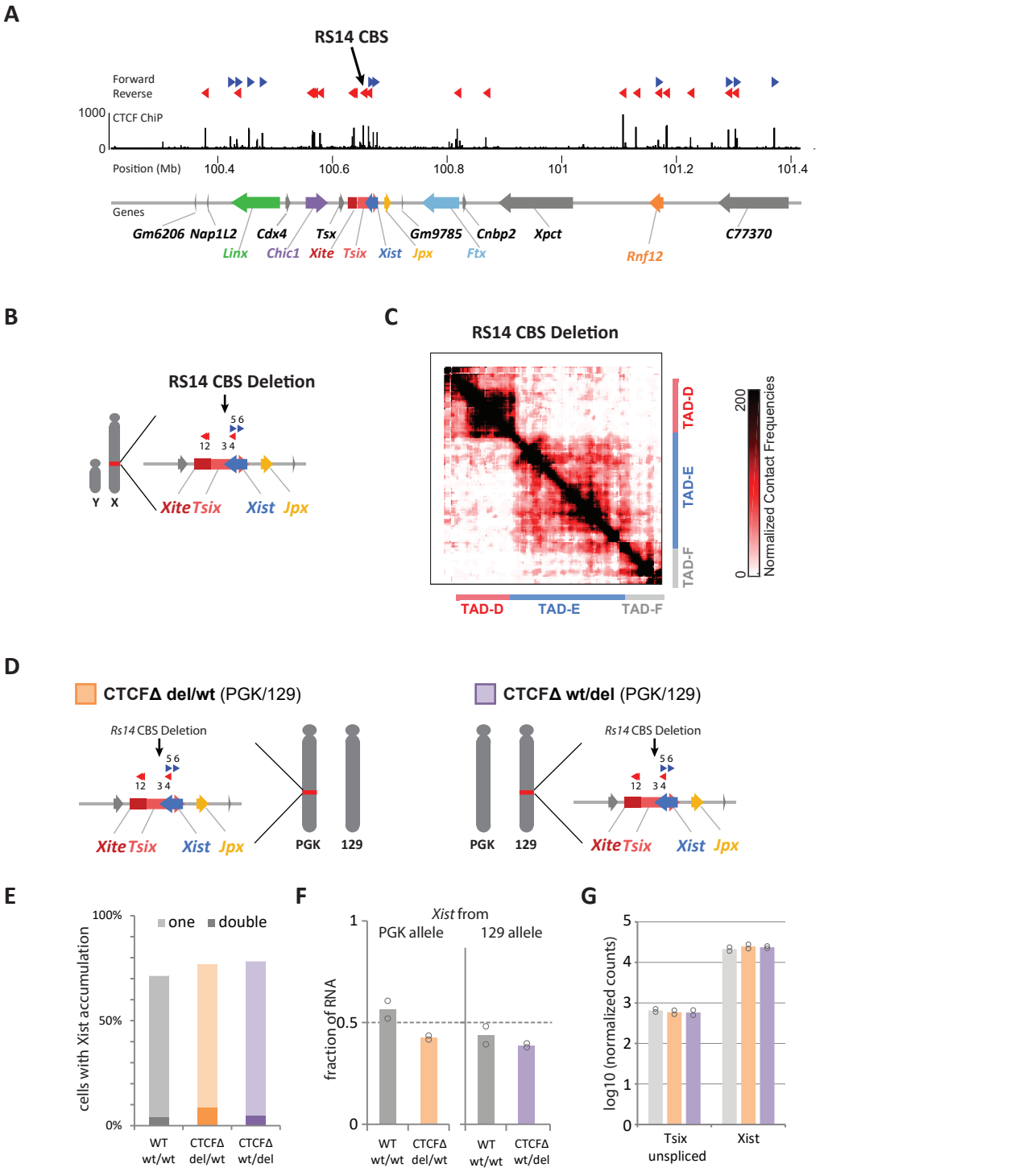
A
RS14 CBS
Forward
Reverse
CTCF ChIP
1000
0
Position (Mb)
100.4
100.6
100.8
101
101.2
101.4
Genes
Gm6206 Nap1L2 Cdx4 Tsx Gm9785 Cnbp2 Xpct C77370
Linx Chic1 Xite Tsix Xist Jpx Ftx Rnf12
B
RS14 CBS Deletion
Y X
Xite Tsix Xist Jpx
C
RS14 CBS Deletion
TAD-D
TAD-E
TAD-F
200
0
Normalized Contact Frequencies
D
CTCFΔ del/wt (PGK/129)
CTCFΔ wt/del (PGK/129)
Rs14 CBS Deletion
PGK 129
E
100%
50%
0%
one double
cells with Xist accumulation
WT wt/wt
CTCFΔ del/wt
CTCFΔ wt/del
F
Xist from
PGK allele
129 allele
fraction of RNA
1
0.5
0
G
log10 (normalized counts)
Tsix unspliced
Xist

Supplementary Fig. 5:

A) Linear visualization of the *Xic* organized into two TADs, as in Fig. 1. CTCF binding sites (CBS) in forward (blue) and reverse (red) orientation, and CTCF ChIP-seq signal from (Nora, Goloborodko et al. 2017). Gene annotation from UCSC RefSeq mm9 (Kent, Sugnet et al. 2002), except for *Xite* (see Methods) and *Linx* (Nora, Lajoie et al. 2012). Black arrow indicates the RS14 CBS.

B) Schematic representation of male mESCs harboring an RS14 CBS deletion.

C) 5C chromosome conformation contact frequencies in male mESCs harboring a deletion of the RS14 CTCF binding site 3' of *Xist*. Map represents pool of two independent mutant cell lines, normalized and binned at 30kb (see Methods). White blocks depict non-mapped sequences. Underneath: the TAD annotation based on wild type 5C data.

D) Schematic representation of female hybrid mESC lines harboring a heterozygous deletion of the RS14 CTCF binding site on either the PGK chromosome (orange) or the 129 chromosome (purple).

E) Efficiency of XCI analyzed by means of RNA-FISH analysis in wild type (grey), deletion/wild type (orange) and wild type/deletion (purple) female epiLSCs at day 4 of differentiation. Bars represent percentage of cells with one (light color) or two (dark color) chromosomes exhibiting *Xist* accumulation or cloud formation, for each independent cell line.

F) Allelic *Xist* expression, measured by pyrosequencing of *Xist* cDNA from female epiLSCs at day 4 of differentiation. Bars represent the fraction of *Xist* mRNA expressed from the PGK (left) or 129 (right) allele in cells with two wild type alleles (grey), in cells with the CTCF deletion on the PGK allele (orange) and cells with the CTCF deletion on the 129 allele (purple). Bars depict the mean of two independent experiments, with dots depicting theindividual experiments. CTCF deletion shows a slight decrease in *Xist* expression in *cis*.

G) nCounter® mRNA expression levels of *Xist* and *Tsix* in female epiLSCs at day 4 of differentiation harboring the CBS deletion on the PGK chromosome (orange) or the 129 chromosome (purple). Bars depict the mean of two independent experiments, with dots depicting the individual experiments.

A

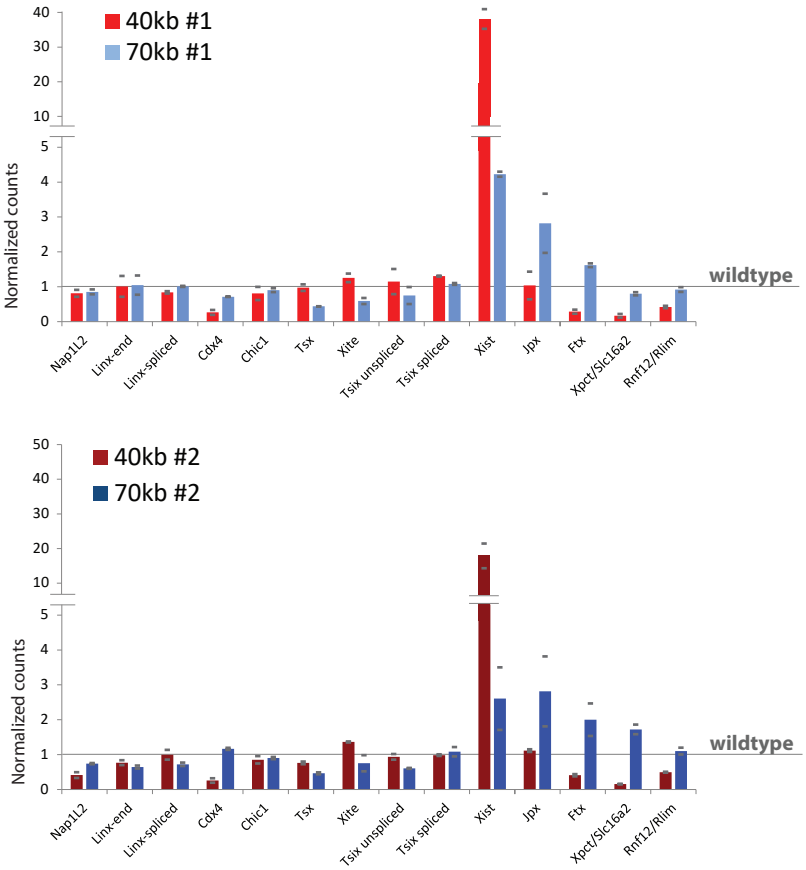

B

Unchanged Downregulated Upregulated according to RNAseq analysis

	Nap1l2	Cdx4	Chic1	Tsx	Xite	Tsix	Xist	Jpx	Ftx	Xpct	Rlim
40kb #1		FDR<0.05					FDR<0.05			FDR<0.05	FDR<0.05
70kb #1							FDR<0.05	FDR<0.05	FDR<0.05		
40kb #2	FDR<0.05	FDR<0.05					FDR<0.05			FDR<0.05	FDR<0.05
70kb #2							FDR<0.05	FDR<0.05	FDR<0.05		

C

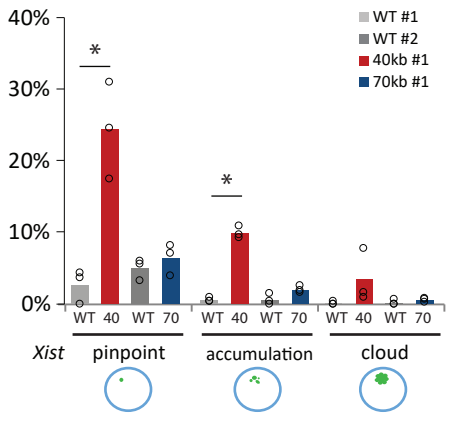

D

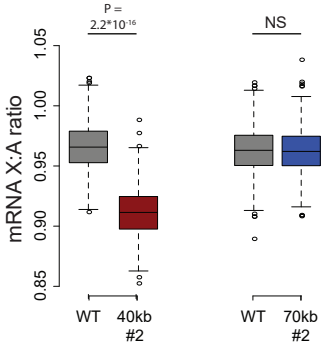

Supplementary Fig. 6:

A) mRNA expression levels from nCounter® analysis in 40kb inversion (red and dark red) and 70kb inversion (blue and dark blue) clones. mRNA levels are normalized to wild type (dashed grey line). Bars depict the mean of two independent experiments, with grey rectangles depicting the individual experiments.

B) Summary of results from differential expression analysis of mRNA sequencing data for genes within the *Xic*. Two independent experiments. Genes significantly upregulated are depicted in red, and genes significantly downregulated in green. Statistical analysis was performed by computing genewise exact tests for differences in the means between two groups of negative binomially distributed counts, and adjusted for multiple testing by Benjamini-Hochberg correction.

C) As in main Fig. 4B. *Xist* accumulation analyzed by RNA-FISH in male wild type (grey & dark grey), 40kb inversion #2 (dark red) and 70kb inversion #2 (dark blue) mESCs. Bars represent percentage of counted cells with either a *Xist* pinpoint, *Xist* accumulation or full *Xist* cloud. For each cell line three independent experiments were performed, each counting from 100 to 400 cells (Supplementary Table 6 for exact sample size details). Dots represent individual experiments. Statistical analysis was performed on independent experiments, using two-sided Fisher's exact test, mutant versus wild type. * = $P < 0.05$ in all three experiments, see Supplementary Table 8 for exact P values.

D) X-linked gene silencing represented by the mRNA expression ratio between X-linked genes and bootstrapped autosomal genes (n=1000). Boxplots represent the median (black line), 25-75% (box) and the minimum and maximum (whiskers) of the bootstrap ratios. Statistical analysis was performed using two-sided Wilcoxon Rank Sum test.

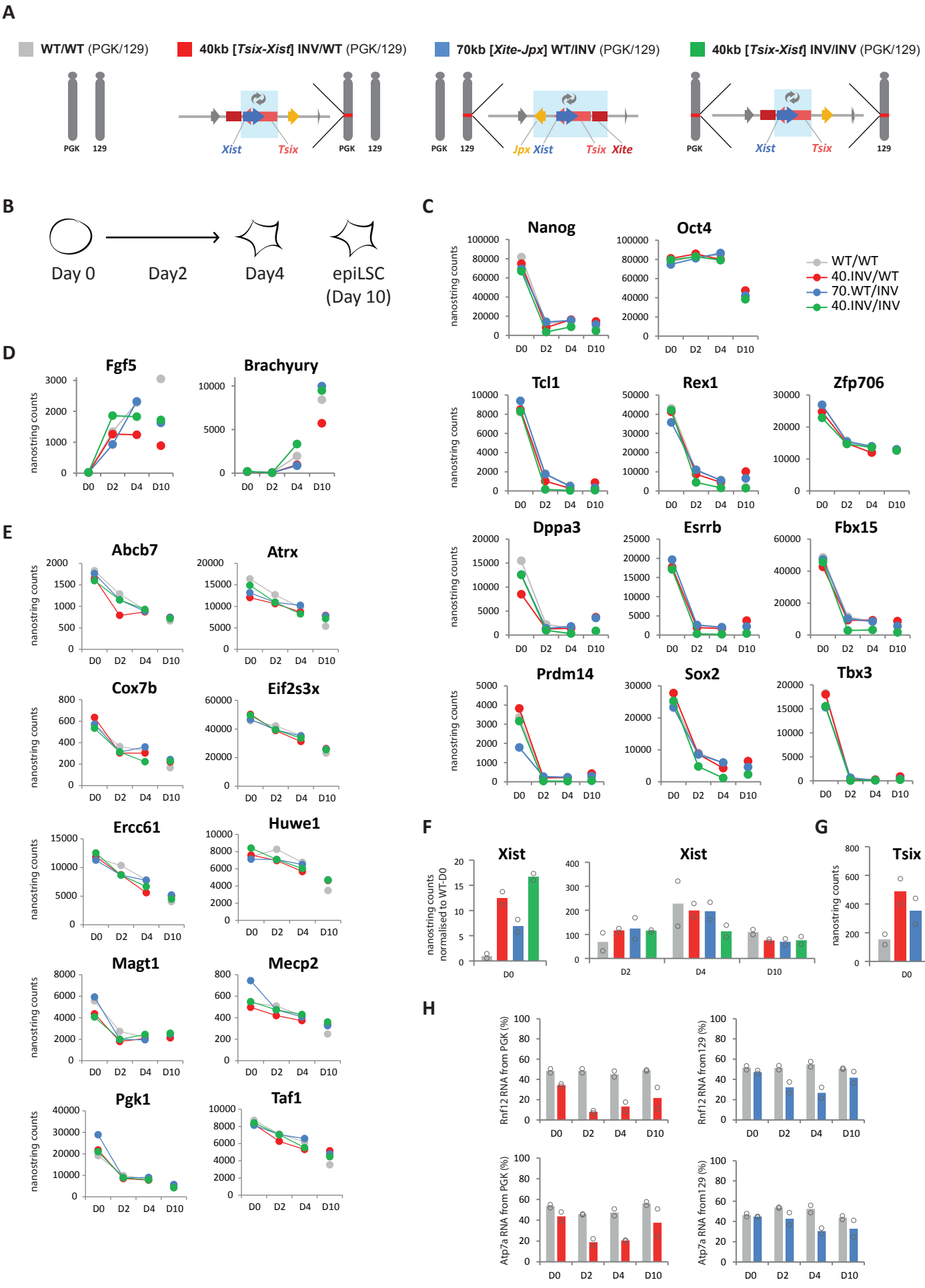
A
WT/WT (PGK/129)
40kb [Tsix-Xist] INV/WT (PGK/129)
70kb [Xite-Jpx] WT/INV (PGK/129)
40kb [Tsix-Xist] INV/INV (PGK/129)
PGK
129
Xist
Tsix
Jpx
Xite
B
Day 0
Day2
Day4
epiLSC
(Day 10)
C
Nanog
Oct4
Tcl1
Rex1
Zfp706
Dppa3
Esrrb
Fbx15
Prdm14
Sox2
Tbx3
nanostring counts
WT/WT
40.INV/WT
70.WT/INV
40.INV/INV
D0
D2
D4
D10
D
Fgf5
Brachyury
E
Abcb7
Atrx
Cox7b
Eif2s3x
Ercc61
Huwe1
Magt1
Mecp2
Pgk1
Taf1
F
Xist
nanostring counts
normalised to WT-D0
G
Tsix
H
Rnf12 RNA from PGK (%)
Rnf12 RNA from129 (%)
Atp7a RNA from PGK (%)
Atp7a RNA from129 (%)

Supplementary Fig. 7:

A) Schematic representation of female hybrid mESC lines harboring a heterozygous 40kb [*Tsix-Xist*] inversion on the PGK chromosome (red), a 70kb [*Xite-Jpx*] inversion on the 129 chromosome (blue) and a homozygous 40kb [Tsix-Xist] inversion (green). Light blue boxes indicate inverted region. The inverted gene localization is shown, compare to Fig. 1B for wild type localizations.

B) Schematic representation of mESC to epiLSC induction, with cell collections at day 0, day 2 and day 4 of early epiLSC induction and an additional collection in epiLSCs that were induced independently for 10 days.

C) nCounter® mRNA expression levels of pluripotency factors and mESC-specific genes in the female cell lines described in A, at 0, 2 and 4 days of mESC into epiLSC induction and in day 10 epiLSCs. Dots depict the mean of two replicates.

D) As in C, for two epiLSC-specific genes.

E) As in C, for X-linked genes normally silenced during epiLSC induction.

F) As in C, global *Xist* expression.

G) As in C, global *Tsix* expression.

H) Allelic *Rnf12* and *Atp7a* expression, measured by a quantification pyrosequencing-based assay of cDNA from female cells at day 0, 2, 4 and 10 of epiLSCs differentiation. Bars represent the percentage of mRNA expressed from the PGK (left) or 129 (right) allele in cells described in A. Bars depict the mean of two replicates.

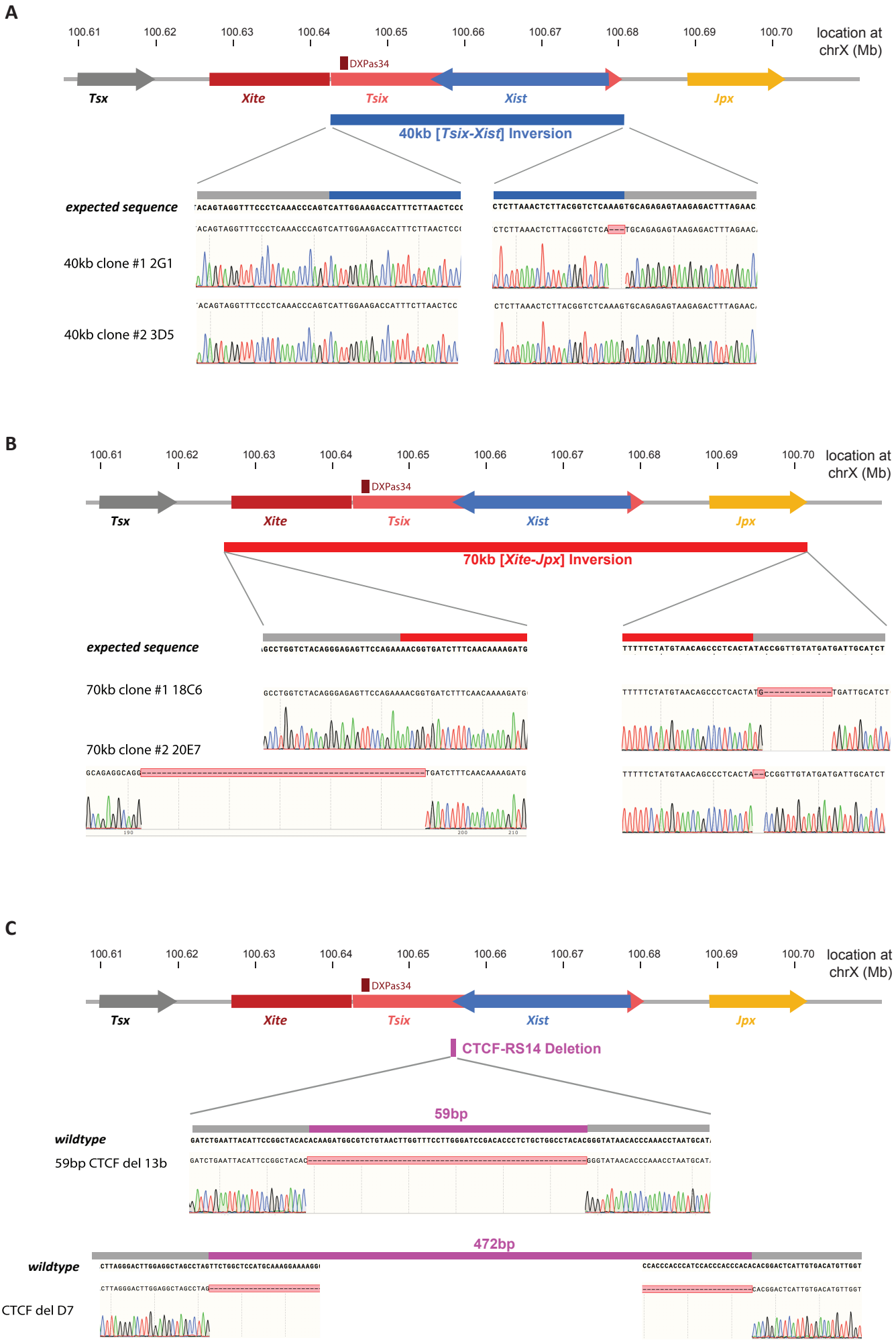
A
100.61
100.62
100.63
100.64
100.65
100.66
100.67
100.68
100.69
100.70
location at chrX (Mb)
DXPas34
Tsx
Xite
Tsix
Xist
Jpx
40kb [Tsix-Xist] Inversion
expected sequence
40kb clone #1 2G1
40kb clone #2 3D5
B
70kb [Xite-Jpx] Inversion
70kb clone #1 18C6
70kb clone #2 20E7
C
CTCF-RS14 Deletion
59bp
wildtype
59bp CTCF del 13b
472bp
472bp CTCF del D7

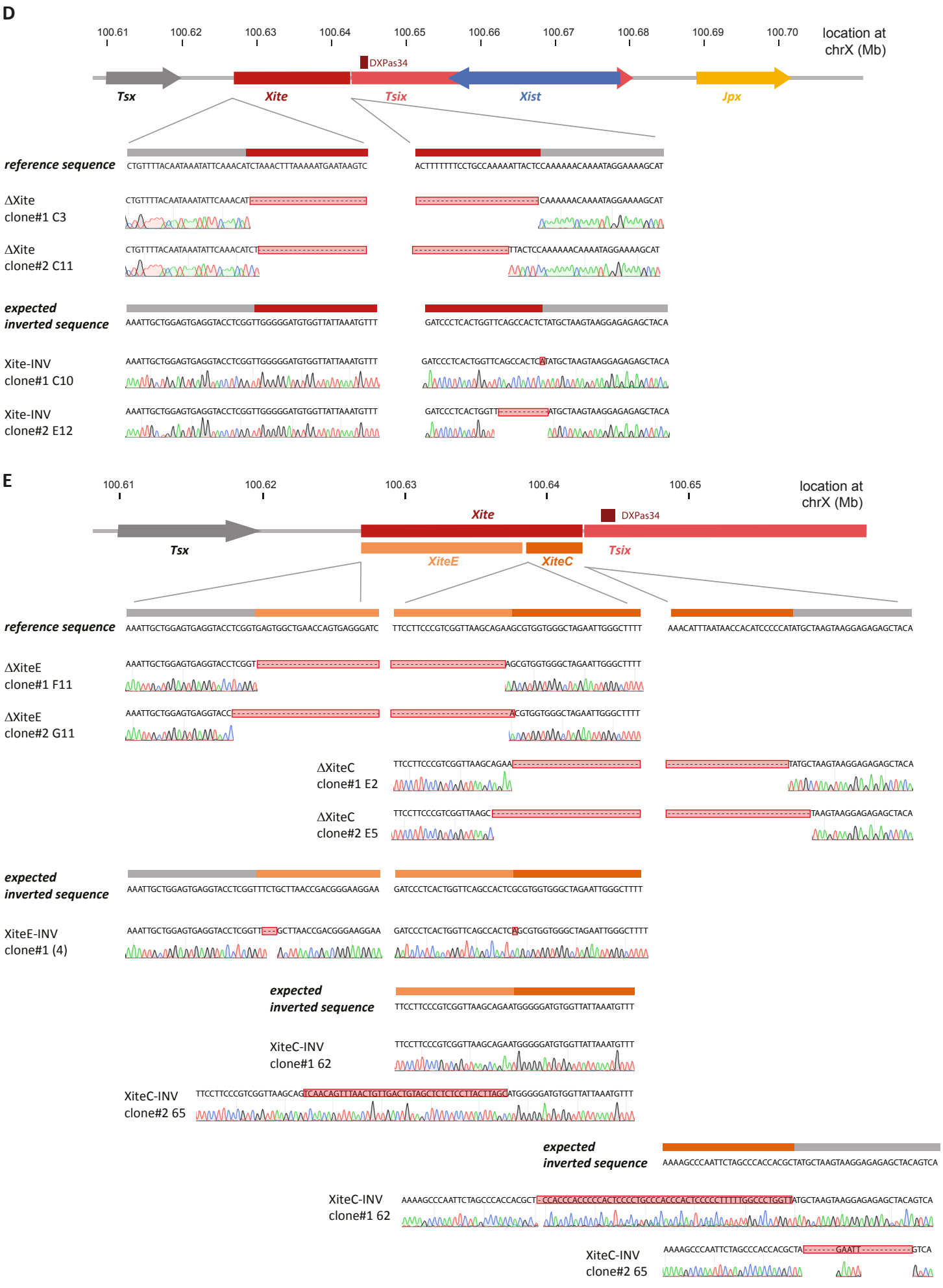
D
100.61
100.62
100.63
100.64
100.65
100.66
100.67
100.68
100.69
100.70
location at chrX (Mb)
DXPas34
Tsx
Xite
Tsix
Xist
Jpx
reference sequence
CTGTTTTACAATAAATATTCAAACATCTAAACTTTAAAAATGAATAAGTC
ACTTTTTTTCCTGCCAAAAATTACTCCAAAAAACAAAATAGGAAAAGCAT
ΔXite clone#1 C3
CTGTTTTACAATAAATATTCAAACAT----------
----------CAAAAAACAAAATAGGAAAAGCAT
ΔXite clone#2 C11
CTGTTTTACAATAAATATTCAAACATCT----------
----------TTACTCCAAAAAACAAAATAGGAAAAGCAT
expected inverted sequence
AAATTGCTGGAGTGAGGTACCTCGGTTGGGGGATGTGGTTATTAAATGTTT
GATCCCTCACTGGTTCAGCCACTCTATGCTAAGTAAGGAGAGAGCTACA
Xite-INV clone#1 C10
AAATTGCTGGAGTGAGGTACCTCGGTTGGGGGATGTGGTTATTAAATGTTT
GATCCCTCACTGGTTCAGCCACTCATATGCTAAGTAAGGAGAGAGCTACA
Xite-INV clone#2 E12
AAATTGCTGGAGTGAGGTACCTCGGTTGGGGGATGTGGTTATTAAATGTTT
GATCCCTCACTGGTT----------ATGCTAAGTAAGGAGAGAGCTACA
E
100.61
100.62
100.63
100.64
100.65
location at chrX (Mb)
Xite
DXPas34
Tsx
XiteE
XiteC
Tsix
reference sequence
AAATTGCTGGAGTGAGGTACCTCGGTGAGTGGCTGAACCAGTGAGGGATC
TTCCTTCCCGTCGGTTAAGCAGAAGCGTGGTGGGCTAGAATTGGGCTTTT
AAACATTTAATAACCACATCCCCCATATGCTAAGTAAGGAGAGAGCTACA
ΔXiteE clone#1 F11
AAATTGCTGGAGTGAGGTACCTCGGT----------
----------AGCGTGGTGGGCTAGAATTGGGCTTTT
ΔXiteE clone#2 G11
AAATTGCTGGAGTGAGGTACC----------
----------ACGTGGTGGGCTAGAATTGGGCTTTT
ΔXiteC clone#1 E2
TTCCTTCCCGTCGGTTAAGCAGAA----------
----------TATGCTAAGTAAGGAGAGAGCTACA
ΔXiteC clone#2 E5
TTCCTTCCCGTCGGTTAAGC----------
----------TAAGTAAGGAGAGAGCTACA
expected inverted sequence
AAATTGCTGGAGTGAGGTACCTCGGTTTCTGCTTAACCGACGGGAAGGAA
GATCCCTCACTGGTTCAGCCACTCGCGTGGTGGGCTAGAATTGGGCTTTT
XiteE-INV clone#1 (4)
AAATTGCTGGAGTGAGGTACCTCGGTT---GCTTAACCGACGGGAAGGAA
GATCCCTCACTGGTTCAGCCACTCAGCGTGGTGGGCTAGAATTGGGCTTTT
expected inverted sequence
TTCCTTCCCGTCGGTTAAGCAGAATGGGGGATGTGGTTATTAAATGTTT
XiteC-INV clone#1 62
TTCCTTCCCGTCGGTTAAGCAGAATGGGGGATGTGGTTATTAAATGTTT
XiteC-INV clone#2 65
TTCCTTCCCGTCGGTTAAGCAGTCAACAGTTTAACTGTTGACTGTAGCTCTCTCCTTACTTAGCATGGGGGATGTGGTTATTAAATGTTT
expected inverted sequence
AAAAGCCCAATTCTAGCCCACCACGCTATGCTAAGTAAGGAGAGAGCTACAGTCA
XiteC-INV clone#1 62
AAAAGCCCAATTCTAGCCCACCACGCT-CCACCCACCCCCACTCCCCTGCCCCACCCACTCCCCCTTTTTGGCCCTGGTTATGCTAAGTAAGGAGAGAGCTACAGTCA
XiteC-INV clone#2 65
AAAAGCCCAATTCTAGCCCACCACGCTA------GAATT----------GTCA

Supplementary Fig. 8:
Sanger sequencing results of the clones generated with following genotypes: **(A)** 40kb [*Tsix-Xist*] inversion, **(B)** 70kb [*Xite-Jpx*] inversion, **(C)** RS14 deletions, **(D)** *Xite* deletions and inversions, **(E)** *XiteE* and *XiteC* deletions and inversions.